LA-UR-80-1649

CONF-800641--5

TITLE: COMPARISON OF FLOW CURVES OF 6061 ALUMINUM ALLOY AT HIGH AND LOW STRAIN RATES

AUTHOR(S): A. E. Carden, M-4, Visiting Staff Member from U. of Alabama
P. E. Williams, M-4, Naval Research Associate
R. R. Karpp, M-4

SUBMITTED TO: International Conference on the Metallurgical Effects Of High Strain-Rate Deformation and Fabrication, Albuquerque, NM, June 1980

MASTER

DISCLAIMER

By acceptance of this article, the publisher recognizes that the U.S. Government retains a nonexclusive, royalty-free license to publish or reproduce the published form of this contribution, or to allow others to do so, for U.S. Government purposes.

The Los Alamos Scientific Laboratory requests that the publisher identify this article as work performed under the auspices of the U.S. Department of Energy.

University of California

LOS ALAMOS SCIENTIFIC LABORATORY
Post Office Box 1663 Los Alamos, New Mexico 87545
An Affirmative Action/Equal Opportunity Employer

DISTRIBUTION OF THIS DOCUMENT IS UNLIMITED

Form No. 836 R3
St. No. 2629
12/78

UNITED STATES
DEPARTMENT OF ENERGY
CONTRACT W-7405-ENG. 36

COMPARISON OF THE FLOW CURVES OF 6061 ALUMINUM ALLOY AT HIGH AND LOW STRAIN RATES

*A. E. Carden**
*P. E. Williams***
R. R. Karpp

Los Alamos Scientific Laboratory
Los Alamos, New Mexico, USA 87545

*Permanent Address - AME Department
University of Alabama
University, Alabama 35486

**Naval Research Associate

Low strain-rate tensile test data (10^{-5} to 10^{-2} s^{-1}) were obtained for 6061 aluminum alloy in the -T6- and -O- condition. Little, if any, strain-rate effect was observed over this range of strain rates. Thirteen expanding ring tests were performed on 1-in.- and 2-in.-diam 6061-T6 and -O- temper rings with maximum strain rates of 3000 to 23000 s^{-1}. The flow stress at 2% circumferential expansion was determined from all of the tests and is shown to be dependent upon maximum strain rate. Furthermore, a size effect is observed, since flow stress at 2% strain and equal strain rates is greater in 2-in. rings than in 1-in. rings. This size effect may be due to shock hardening, but a definite conclusion has not yet been reached. The -T6- temper rings also show a size effect, but the difference between the 1- and 2-in. rings was not the same for all values of flow stress.

I. INTRODUCTION

In the design of dynamically loaded structures, there is a need to know the functional relationship between stress, strain, and strain rate for the materials under consideration. The centric, axial loading of a smooth, straight solid bar is a reference test, the results of which can be used as a basis for

predicting the behavior of structural elements under other states of stress. These reference tests, called tension tests, are usually performed at low, constant rates of displacement. The laboratory tensile test is the primary source of materials behavior for monotonic loading. From the load and displacement data, a "flow curve" (stress vs strain) is derived and several mechanical properties are determined.

Of particular interest is the stress value at which plastic flow becomes significant. There are various methods and labels used for this yield condition or flow stress. This stress is dependent on several factors: namely, the material, its prior thermal-mechanical history, test temperature, strain rate, and stress state.

To continue the plastic deformation process, the stress must increase. This process of strain hardening continues until fracture terminates the process. In uniaxial loading, the geometric instability of necking modifies the plastic deformation process and the terminal condition is fracture.

There is a deficiency in our knowledge of materials behavior, however, in that the flow curve and mechanical properties of materials at high strain rates are not commonly available. Moreover, high strain rate testing cannot be performed in the usual tensile testing machine. The expanding ring test (1) subjects an expanding ring to uniaxial loading, and the stress-strain function can be obtained from the radial-velocity versus time function (V-t). Although the strain rate varies during an expanding ring test, the technique does offer a potential for studying strain-rate effects, since several experiments can be used to develop a stress-strain-strain rate relationship (1). The object of this paper is to present stress-strain data for 6061 aluminum alloy from both the low strain-rate tension test and the high strain-rate expanding ring test. The results are analyzed to determine the effect of strain rate on the yield condition. Furthermore, two mathematical models that have been used to describe the flow curve are used for tensile test data analysis. The stress-strain data used in the analysis are limited to strains up to the necking strain, since beyond that point, uniaxial stress conditions no longer exist.

II. EXPERIMENTAL PROCEDURE

The test method for the expanding ring is described in (1). The 6061 rings were machined from 6061-T6 plate. The ring specimen dimensions were (a), 2.00 in. i.d., 2.125 in. o.d., 0.25 in. high, and (b) 1.00 in. i.d., 1.0625 in. o.d., and 0.125 in. high. The 2 in. i.d. rings are identical to those described in (2). The

specimen diameters were measured post-test to determine the final inelastic circumferential strain. Initially, the rings had about 0.006 in. and 0.003 in. diametral interference to insure good contact between driver and ring. Heating the ring to 350°F allowed a shrink fit.

The tensile tests were performed with both an Instron and a MTS testing machine. The Instron tests had a controlled constant crosshead speed, with strain rates varying from 10^{-5} to 10^{-2} s^{-1}. The strain rates in the MTS tests were controlled and varied from 10^{-5} to 10^{-2} s^{-1}. The sheet-type test specimens had uniform gauge dimensions of 0.0625 in. thick, 0.50 in. wide, and 2.5 in. long. These specimens were blanked from 6061-T6 sheet as 9 in. by 0.75 in. coupons in the transverse direction and template-milled in a TensilKut machine to a standard ASTM tensile specimen dimension. A one-inch gauge length extensometer was used in all MTS tests and the load-elongation recorded on a X-Y recorder. No extensometer was used for the tests in the Instron. Crosshead motion was recorded on a strip chart and an effective gauge length was used to convert the inelastic deformation to inelastic strain. The tensile tests were generally terminated shortly after the maximum load was reached. Only data up to the maximum load were used to determine the flow curve.

III. RESULTS AND DISCUSSION

Load as a function of strain (P vs $\Delta L/L_0$) from the tensile tests are shown in Figures 1 and 2 for strain rates from 10^{-5} to 10^{-2} s^{-1}. These data were converted to true stress-true strain and are plotted logarithmically in Figure 3. The -T6- temper data can be described by a power function

$$\epsilon_p = \left(\frac{\sigma}{B}\right)^{\frac{1}{n}} \quad , \qquad [1]$$

where B = 61 ksi, and n = 0.05428. The -O- temper data are better described by a Voce equation (4),

$$\epsilon_p = \epsilon_c \ln\left(\frac{\sigma_\infty - \sigma_0}{\sigma_\infty - \sigma}\right) \quad , \qquad [2]$$

where ϵ_c = 0.037, σ_∞ = 26 ksi, and σ_0 = 9 ksi. These equations fit the data reasonably well over the range 10^{-5} to 10^{-2} s^{-1}. The homologous temperature, i.e., the ratio of the temperature to the melting point temperature in degrees K, is about 0.33 and one would expect small, if any, viscoelastic effects in these test periods. The flow curves for these tensile tests have almost as

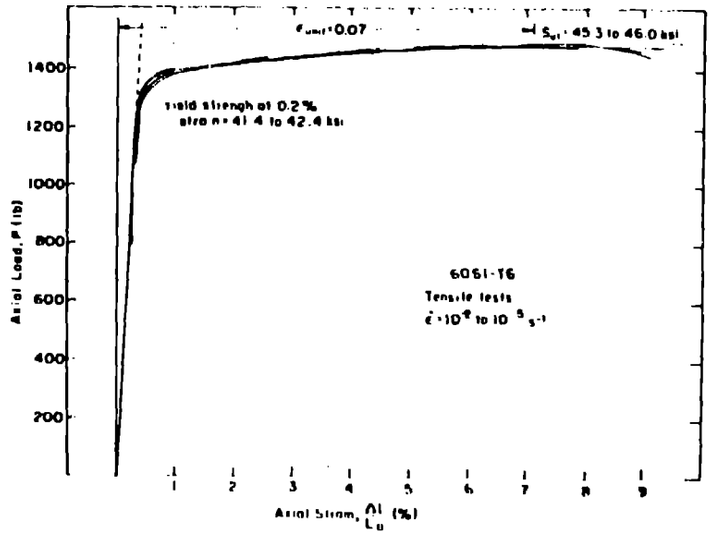

FIGURE 1. Load-elongation curves from tensile tests on 6061-T6 aluminum alloy. Area = 0.0324 in.^{2}; $10^{-5}<\dot{\epsilon}<10^{-2}$ s^{-1}; temperature = 20°C. ϵ_{uni} is the plastic strain at maximum load. S_{ut} is the maximum load divided by the original area.

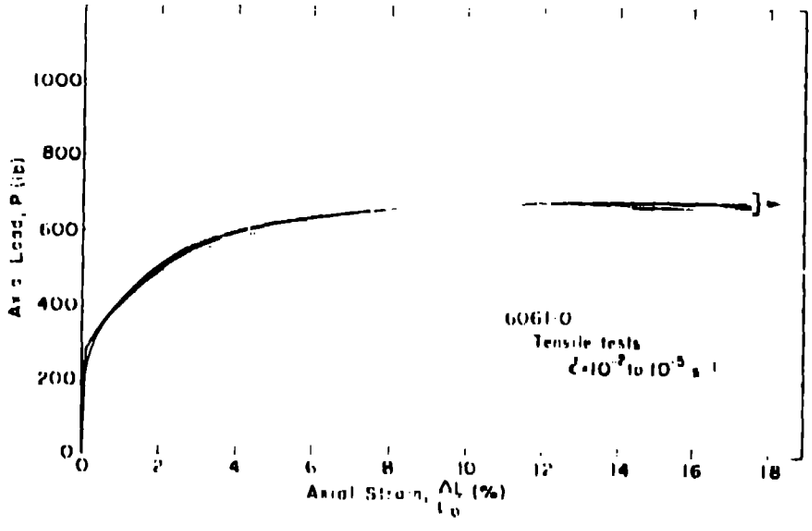

FIGURE 2. Load-elongation curves from tensile tests on 6061-0 aluminum alloy. Area = 0.0324 in.^{2}; $10^{-5}<\dot{\epsilon}<10^{-2}$ s^{-1}; temperature = 20°C.

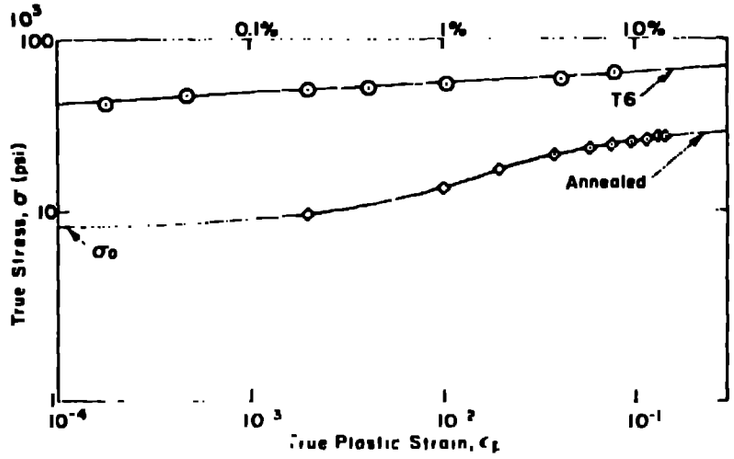

FIGURE 3. True stress-true strain curves from tensile tests on 6061-T6 and -O aluminum alloys.

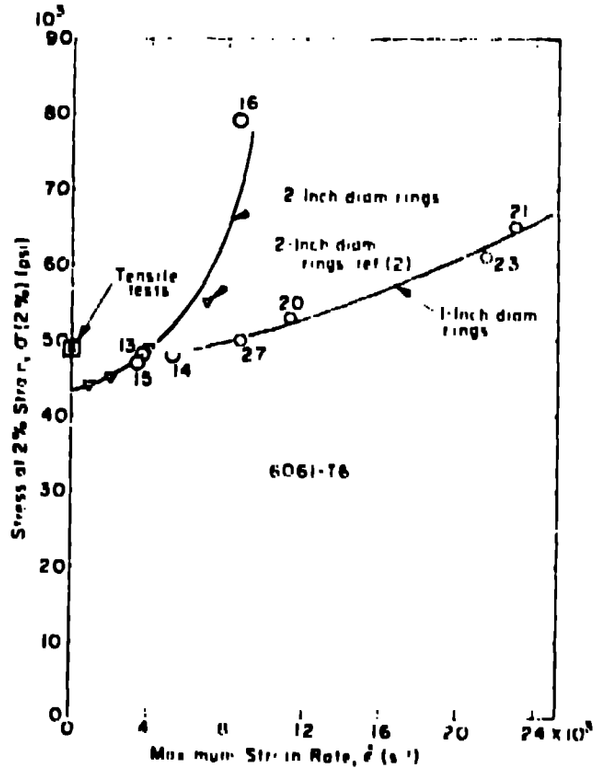

FIGURE 4. Flow stress at 2% strain as a function of plastic strain rate for 6061-T6 expanding rings.

much scatter in replicate tests (at 10^{-3} s^{-1} we performed seven replicate tests) as there is between the flow curves at different strain rates. At least two tests were performed at each strain rate. The heat of the material (i.e., chemistry of the original ingot) and product form (sheet vs plate) were different for the tensile and expanding ring specimens. The tensile test data, therefore, are most valuable for determining if there are strain-rate effects at the low strain rates. The absolute value of the flow stress may be different for the ring and tensile specimens at the same strain rate. The strain at the maximum load (i.e., the uniform strain, ε_{unif}) was from 0.06 to 0.08 for the -T6- and from 0.16 to 0.20 for the -O- temper.

Results from 13 expanding ring tests are shown in Table I. The maximum strain rate is that determined at the maximum velocity

$$\dot{\varepsilon}_{max} = \frac{V_{max}}{r_0} \quad . \qquad [3]$$

The time period, Δt^*, required for the velocity to become zero must be estimated in some cases because the laser velocity interferometer record (V-t) becomes noisy before the ring velocity decreases to zero. In some cases, the cause of the noise is believed to be the fracturing of the specimen and/or driver before the end of the expansion of the ring. The V-t data are invalid after that event. We have chosen to extrapolate the V-t curve to zero velocity to estimate this time period. The value of stress at 2% strain and at an arbitrary strain-rate ($\dot{\varepsilon}_{max}$), is used as an index of the flow stress and is determined from the V-t diagram and the equations of motion of the ring as the stress

$$\sigma(2\%) = -\rho r_0 \, (1.02) \left(\frac{dV}{dt}\right)_{\varepsilon = 2\%} \quad . \qquad [4]$$

The time period for this 2% strain to occur is approximately

$$t_{2\%} = \Delta t^* \left(1 - \sqrt{1 - \frac{(0.04) r_0}{(V_{max}) \Delta t^*}}\right) \quad . \qquad [5]$$

There are several reasons for using σ at $\varepsilon = 2\%$ as the correlating parameter for strain-rate effects. The complete flow curves derived from the V-t data were not available for about one-half of the tests because of driver failure or loss of the interferometer record. Data out to about 10 μs were obtained and the initial stress and strain values were determined, but the flow curve and the hardening characteristics were only available for about one-half of the tests; the V-t data contain large oscillations of velocity during the first several microseconds. These oscillations are due to radial waves in the ring. Even though the

TABLE I

EXPANDING RING - 6061 ALUMINUM

$\rho = 2.70\ g/cm^3$, $C_0 = 5328\ m/s$
$C = 0.104\ cal/g$, $E = 6.96\ 10\ dynes/cm^2$

Test No. 25XX	Temper	Nom Diam (in.)	MAX Vel (m/s)	$\dot{\varepsilon}$ Max (s^{-1})	Δt* (μs)	σ at (2%) (ksi)	ε_f (%)
13	-T6-	2	99	3.7×10^3	23	48	3.3
15	-T6-	2	96	3.6	22	47	3.2
14	-T6-	2	140	5.2	32	48	5.2
16	-T6-	2	218	8.6	*20	79	**
20	-T6-	1	153	11.3	16	53	8.0
21	-T6-	1	310	22.9	*10	65	**
23	-T6-	1	290	21.6	*18	61	**
27	-T6-	1	118	6.7	13	50	5.7
18	-O-	2	79	2.9	41	21	4.6
17	-O-	2	160	5.9	*12	34	13.7
19	-O-	1	134	9.9	*12	26	15.7
22	-O-	1	310	23.0	* 6	89	**
26	-O-	1	104	7.7	*14	16	4.3

*Interferometer record available to time shown.
**Driver fractured subsequently destroying specimen.

displacements are extremely small, the velocity changes at the ring surface, as determined by the interferometer records, are significant. Consequently, an accurate determination of the stress in this region cannot be made. Because the primary interest in ring behavior is the plastic deformation of from 1% to the condition of necking, and because this alloy has a relatively "flat" flow curve after about 1%, σ (2%) is a reasonable measure of the strength level of the material for plastic deformation.

The final strain values ε_f were obtained from the tested rings by measuring the final diameter and using the relation

$$\varepsilon = \ln\left(\frac{D_f}{D_o}\right) , \qquad [6]$$

where D_f and D_o are the final and initial diameters, respectively. The maximum radial displacement can be determined from the V-t function by

$$\Delta r = \int_{t=o}^{t=\Delta t^*} V dt , \qquad [7]$$

and the final strains are consistent with [6] where

$$\varepsilon_{max} = \ln\left(1 + \frac{\Delta r}{r_o}\right) . \qquad [8]$$

The values of stress at 2% strain, σ (2%), are plotted versus maximum strain rate in Figures 4 and 5. The tensile test values are shown for comparison. The flow stress for the -T6- temper is about 27 ksi greater than that for the -O- temper at low strain rates. Data for the -T6- temper (Figure 4) are shown with data from Hoggatt and Recht (2) who also tested 6061-T6 with 2-in.-diam rings. Our data compare well with theirs. Small, if any, strain-rate effects are seen in the region of 4000 s^{-1} and below. Above this strain rate, however, we observe a difference between the 1-in.-diam rings and the 2-in. ones. Our tentative understanding of this phenomenon is that some shock hardening occurs in the material during the kick-off and early ringing of the radial wave in the ring. For the same maximum strain rate, the intensity of the shock in the 1-in.-diam rings is about one-half that in the 2-in. rings. In Figure 5, for example, for equal values of σ (2%), the strain rate in the 1-in.-diam rings is twice as great as the strain rate in the 2-in. rings. These two rings have about the same maximum velocity and approximately the same shock intensity. Consequently, the data show a size effect. The size effect in the annealed material (Figure 5) is different from that in the -T6- material (Figure 4). We plan additional experiments to study this phenomenon.

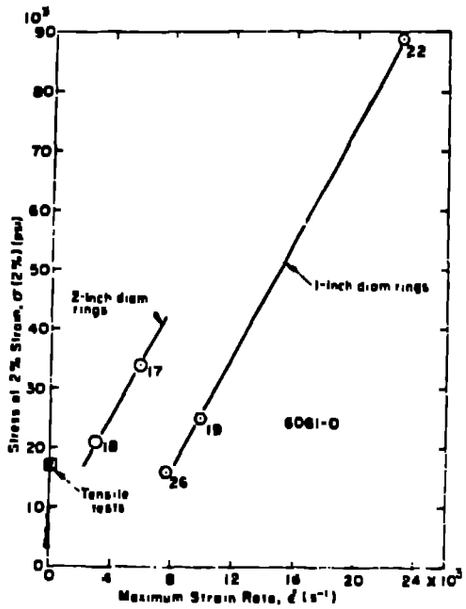

FIGURE 5. Flow stress at 2% strain as a function of maximum strain rate for 6061-O expanding rings.

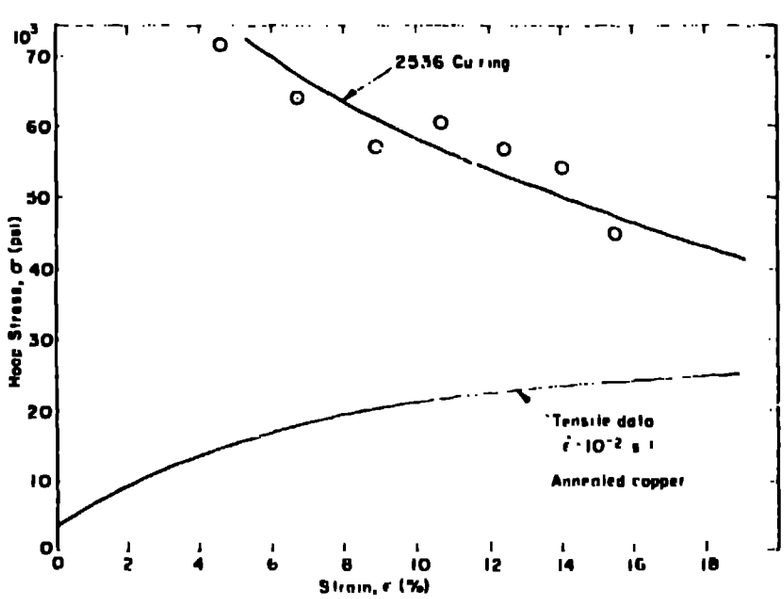

FIGURE 6. Stress-strain curves for annealed copper obtained from a low strain-rate tensile test and a high strain-rate expanding ring test.

In tests of annealed copper rings where we have several complete V-t curves, we have observed a large σ (2%) at the beginning of the deformation followed by a decreasing stress during the subsequent deformation. One set of these data are shown in Figure 6. The V-t curve for this annealed copper 2-in.-diam sample is shown in Figure 5(a) of Reference (1). The quasi-static tensile flow curve is given in Figure 6 for comparison. The strain rate decays from 4.85 to 2.45 (10^3) s^{-1} during the expansion shown. If the increase in σ (2%) were due only to shock hardening, one would not expect to see the decay in stress during the expansion of the copper rings.

The stress, σ (2%), shown for Test No. 2516, Figure 4, is greater than the ultimate tensile strength of the material, but the ultimate tensile strength value is not a value representing fracture; rather, it is a condition representing the initiation of a geometric instability. In the expanding rings, the 2% deformation is so small that the condition of necking is not present. We, therefore, postulate that there are several phenomena that interact to raise the flow stress, σ (2%), for the expanding ring: one is a true strain-rate effect in the material; another is a geometric and/or shock-hardening effect. There may be others.

The flow stress σ (2%) values for the -O- temper rings are shown in Figure 5. Again, as in Figure 4, we observe a difference in the relation between the flow stress and strain rate for the 2-in.- and 1-in.-diam rings. Furthermore, the rate of change of σ (2%) with strain rate is much more pronounced for the annealed alloy than it is for the -T6- temper. The results from specimen 22 are rather convincing, in that specimens 26, 19, and 22 yield data that are consistent and have large changes in the σ (2%) values with increasing strain rate. The 2-in.-diam rings show the same trend, but we lack data for strain rates greater than 5200 s^{-1}. The observation that the rate of increase of σ (2%) with strain rate is much more pronounced in the -O- temper than in the -T6- temper suggests that shock hardening may be present.

We have also considered the effect of temperature on the flow curve. Thermal effects can arise from two sources—shock-wave heating and plastic-deformation heating. The maximum possible temperature rise resulting from the plastic deformation is

$$\Delta T_{max} = (\int \sigma d\epsilon_p)/\rho C \quad , \qquad [9]$$

where C is the heat capacity and ρ is the mass density.

For an aluminum ring expanding to 10% at a stress level of 40 ksi, the temperature rise is about 24°C. In slow strain-rate tensile testing, the flow stress would show a small decrease with

a 24°C temperature increase. The shock induced temperature would rise early and persist; the thermal rise due to plastic deformation would monotonically increase throughout the test. A temperature increase would lower the yield strength.

The expanding ring data of Hoggatt and Recht (2), shown in Figure 4, were derived from ring-driver configurations that were identical to our 2-in. rings. Their test results were obtained from a streak camera and produced displacement-time functions. In order to determine the stress, the data had to be differentiated twice. In order to circumvent the double differentiation of experimental data, a parabolic form was assumed for the displacement-time function. Such a function would be obtained from a linear V-t function. In our 6061 experiments, we observed V-t functions that are nearly linear.

Other ring tests on 6061-T6 rings were reported by Walling and Forrestal (3), but these rings were larger (6-in. diam) and loaded by a short duration magnetic pressure pulse, the strain being measured by a strain gauge cemented to the outer surface of the ring. The strain signal was perturbed by strong magnetic field interference during the first 20 μs of expansion. The stresses were calculated from current measurements in the ring and the driver coil. The maximum strain rates were about 1000 s^{-1}; only one test result is given and no stresses are reported.

A sample V-t relationship taken from Test 2515 is shown in Figure 7, and the integrated V-t function (radial displacement) is shown in Figure 8. Taking the mean value of V_{max} during the early oscillation to be 96 m/s and the time duration Δt^* of 22 μs to decelerate to zero velocity yields an average deceleration of 4.36 10^6 m/s^2. The strain at the line marked 10 μs is about 2% (radial displacement of 0.586 mm) and the time of expansion is 7.4 μs. The stress at this point is calculated to be 47 ksi. An error of 1° on the slope of the V-t function will cause an error in the calculated stress of 4% or about 2 ksi.

The vibration in the early expansion, marked H, shows a transit time of the wave across the ring of about 0.33 μs. The transit time of an elastic wave is 0.298 μs taking C_0 in aluminum as 5.328 km/s. The multiple reflections of this radial wave may influence the local yield condition, change the dislocation density of the material, heat the sample, and possibly cause other phenomena. It is obvious that the reflections affect the initial velocity-time profile. In aluminum, the wave dampens out in about 4.7 μs (about 13.5 transits across the ring). By this time, the ring has expanded about 1% and is well into the plastic regime in the circumferential strain process. The deceleration is approximately constant for about another 17.5 μs. Even though the deceleration is approximately constant, the stress increases

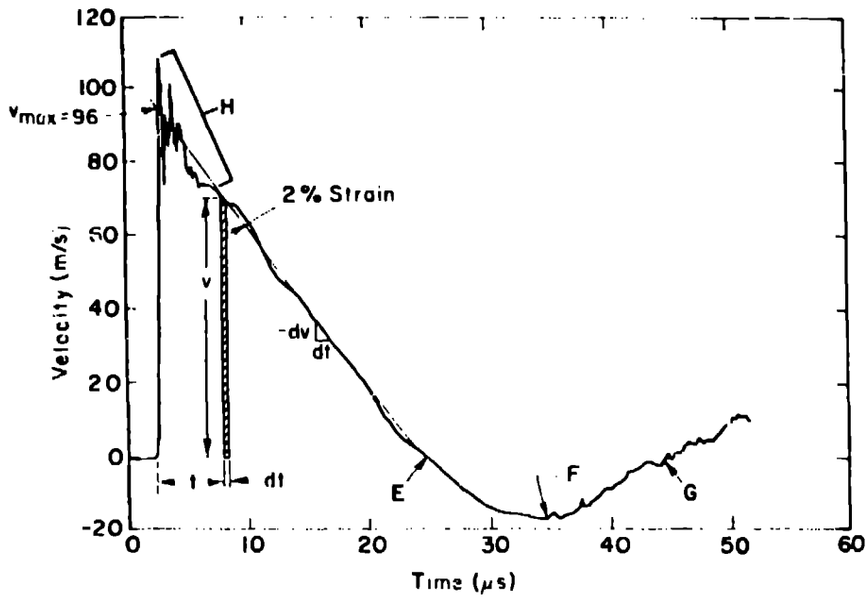

FIGURE 7. Velocity-time curve for expanding ring Test No. 2616.

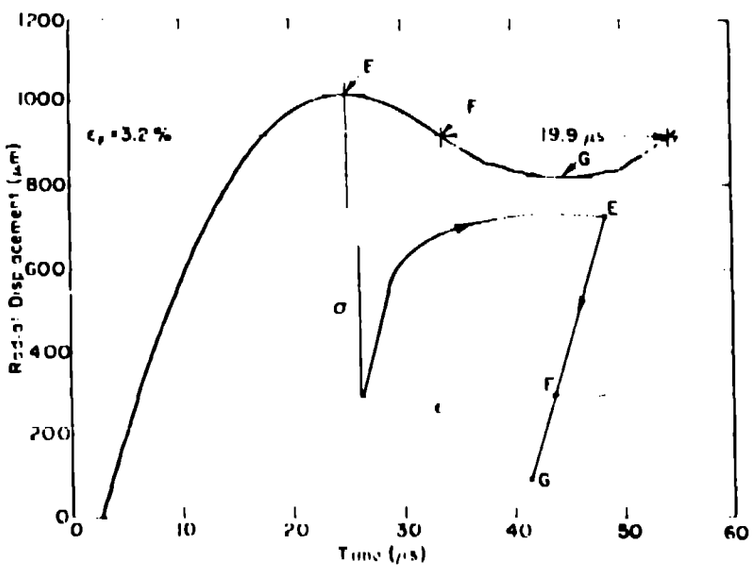

FIGURE 8. Displacement-time curve for expanding ring Test No. 2616

because it depends on the instantaneous radius, r, which increases. For this test, the maximum radial expansion is 1.06 mm as determined from the integral of the V-t diagram. This produces a strain of 3.9%, which includes 0.3% elastic strain. The strain calculated from the diameter at the end of the test was 3.2% ± 0.5%.

At "E", shown in Figures 7 and 8, the outward radial velocity is zero, but the ring still has stored elastic strain energy. The ring elastically rebounds to point "F". At this point, the velocity is 16.5 m/s and the inward radial displacement is 0.082 mm. This corresponds to a strain of 0.0288 or a stress of about 29 ksi at "E". Setting the kinetic energy at 16.5 m/s equal to the stored strain energy, a hoop stress of 31.4 ksi is obtained. The observed period of oscillation is 39.8 μs. The period of natural vibration is proportional to r, E, and ρ, and is given by

$$\text{period} = 2\pi r \sqrt{\frac{\rho}{E}} \quad . \qquad [10]$$

The calculated time period is 35 μs or a frequency of 29 kHz. These and other comparisons indicate that the interferometer measurements of velocity time and the assumptions of motion of the ring are valid.

A computer program was written to reduce the V-t data to stress-strain-strain rate values. Also, a Voce equation (4), with strain-rate- and temperature-dependent parameters was incorporated into the program to parameterize the flow curve. The program iterated until the parameters, which minimized the difference between the stress-strain values derived from the V-t data and those calculated from the computer-determined Voce equation, were calculated. The tensile test stress-strain results show that a power function better describes the -T6- flow curve, and this function will be used in future analyses. The first program had, as input, the digitized V-t data. The interferometer is so sensitive that minute surface disturbances (possibly associated with surface rumpling that accompanies plastic deformation) produce small, short duration, perturbations in the V-t record. These disturbances are of such short duration that they are not visible in the integrated V-t function, i.e., the displacement time, but they do produce large changes in the instantaneous derivative, and, consequently, the hoop stress. Smoothing techniques are being implemented into the program. We are continuing work on data reduction, selection of appropriate constitutive equations, and determination of the strain-rate-dependent parameters in the equations.

Tests 17, 19, and 20 were all strained to deformations that were larger than the instability strain associated with the

tension test. Specimen 20 had the beginning of four necks. These local necks were in the initial stages, not as severe as those in the tension tests. It is significant that they had begun and that there were more than one. Any unloading that accompanies the initiating neck requires a significant time to be sensed by material remote from the neck. The transit time for an elastic wave to travel one-half the circumference is 7.5 μs and 15 μs for the 1- and 2-in. rings, respectively. Many of the samples had surface rumpling. The V-t record shows all of the ring motion, including the minor surface perturbations that occur on the surface where the beam is focused.

IV. CONCLUSIONS

From the data presented in this report, strain rate and size effects are found for 6061 aluminum expanding rings. Strain rates of up to 23,000 s^{-1} have been produced. The geometric (size) effect may be related to shock hardening. The data from our 6061-T6, 2-in.-diam rings agree well with similar data published in the literature. The strain-rate effect is not appreciable in this alloy at strain rates below 2000 s^{-1}.

V. ACKNOWLEDGEMENTS

The authors gratefully acknowledge the contributions of Thomas Gould and Elaine Alei of the Los Alamos Scientific Laboratory for conducting the ring tests and reducing the data, and of Rodney Young and Michael Pope of the University of Alabama for the performance and data reduction of the tensile tests.

VI. REFERENCES

1. Warnes, R. H. et al, "An Improved Technique for Determining Dynamic Material Properties Using the Expanding Ring," this conference.
2. Hoggatt, C. R., and Recht, R. F., "Stress-Strain Data Obtained at High Rates Using an Expanding Ring," *Exp. Mech.*, 9, 441 (1969).
3. Walling, H. C., and Forrestal, M. J., "Elastic-Plastic Expansion of 6061-T6 Aluminum Rings," *AIAA J.*, 11, N8, 1196 (1973).
4. Voce, E., "A Practical Strain-Hardening Function," *Metallurgia*, 51, N307, 219 (1955).